

Video Article

# Preparation of Polyoxometalate-based Photo-responsive Membranes for the Photo-activation of Manganese Oxide Catalysts

Akira Yamaguchi<sup>1,5</sup>, Toshihiro Takashima<sup>2</sup>, Kazuhito Hashimoto<sup>1,6</sup>, Ryuhei Nakamura<sup>3,4</sup>

<sup>1</sup>Department of Applied Chemistry, The University of Tokyo

<sup>2</sup>Clean Energy Research Center, University of Yamanashi

<sup>3</sup>Biofunctional Catalyst Research Team, RIKEN Center for Sustainable Resource Science

<sup>4</sup>Earth-Life Science Institute (ELSI), Tokyo Institute of Technology

<sup>5</sup>Department of Materials Science and Engineering, Tokyo Institute of Technology

<sup>6</sup>National Institute for Materials Science

Correspondence to: Akira Yamaguchi at [ayamaguchi@ceram.titech.ac.jp](mailto:ayamaguchi@ceram.titech.ac.jp)

URL: <https://www.jove.com/video/58072>

DOI: [doi:10.3791/58072](https://doi.org/10.3791/58072)

Keywords: Chemistry, Issue 138, Polyoxometalate, metal-to-metal charge transfer, artificial photosynthesis, manganese oxide, oxygen evolution, product separation

Date Published: 8/7/2018

Citation: Yamaguchi, A., Takashima, T., Hashimoto, K., Nakamura, R. Preparation of Polyoxometalate-based Photo-responsive Membranes for the Photo-activation of Manganese Oxide Catalysts. *J. Vis. Exp.* (138), e58072, doi:10.3791/58072 (2018).

## Abstract

This paper presents a method to prepare charge-transfer chromophores using polyoxotungstate ( $PW_{12}O_{40}^{3-}$ ), transition metal ions ( $Ce^{3+}$  or  $Co^{2+}$ ), and organic polymers, with the aim of photo-activating oxygen-evolving manganese oxide catalysts, which are important components in artificial photosynthesis. The cross-linking technique was applied to obtain a self-standing membrane with a high  $PW_{12}O_{40}^{3-}$  content. Incorporation and structure retention of  $PW_{12}O_{40}^{3-}$  within the polymer matrix were confirmed by FT-IR and micro-Raman spectroscopy, and optical characteristics were investigated by UV-Vis spectroscopy, which revealed successful construction of the metal-to-metal charge transfer (MMCT) unit. After deposition of  $MnO_x$  oxygen evolving catalysts, photocurrent measurements under visible light irradiation verified the sequential charge transfer,  $Mn \rightarrow MMCT \text{ unit} \rightarrow \text{electrode}$ , and the photocurrent intensity was consistent with the redox potential of the donor metal (Ce or Co). This method provides a new strategy for preparing integrated systems involving catalysts and photon-absorption parts for use with photo-functional materials.

## Video Link

The video component of this article can be found at <https://www.jove.com/video/58072/>

## Introduction

The development of solar energy conversion systems using artificial photosynthesis or solar cells is necessary to enable the provision of alternative energy sources that can ameliorate global climate and energy issues<sup>1,2,3,4</sup>. Photo-functional materials can be broadly categorized into two groups, semiconductor-based systems and organic molecule-based systems. Although many different system types have been developed, improvements still need to be made because semiconductor systems suffer from a lack of precise charge transfer control, and organic molecule systems are not adequately durable with respect to photo-irradiation. However, the use of inorganic molecules as charge transfer unit components can improve these respective issues. For example, Frei *et al.* developed oxo-bridged metal systems grafted on the surface of mesoporous silica which can induce the metal-to-metal charge transfer (MMCT) by photo-irradiation and trigger photochemical redox reactions<sup>5,6,7,8,9</sup>.

Our group extended the single atomic system to a polynuclear system utilizing polyoxometalate (POM) as the electron acceptor<sup>10,11,12</sup>, with the expectation that use of the polynuclear system would be advantageous in the induction and control of the multi-electron transfer reaction, which is an important concept in energy conversion. In the protocol described here, we present the detailed method used to prepare the POM-based MMCT system, which works in a polymer matrix as we recently reported<sup>13</sup>. The membrane-type configuration is favorable for product separation between anodic and cathodic reaction products. The cross-linking method was applied, which enabled formation of a self-standing membrane, even with high POM contents. Photoelectrochemical measurements proved that appropriate selection of the donor metal is key to triggering the target. The POM/donor metal system works as a photo-sensitizer to activate multi-electron transfer catalysts under visible light irradiation. Although this work utilizes  $MnO_x$  as a multi-electron transfer catalyst for the water oxidation reaction, this photo-functional system is also applicable for use with other types of reactions by utilizing various POMs, donor metals, and catalysts.

## Protocol

It is advisable to refer to all relevant material safety data sheets (MSDS) prior to using chemicals, as some used in these syntheses are highly acidic and corrosive. In addition, one polymer used in this work (polyacrylamide) may contain the carcinogenic monomer, acrylamide. The use of personal protective equipment (safety glasses, gloves, lab coat, full-length pants, closed-toe shoes) is required to prevent injuries from chemicals or heat. After conducting the cross-linking process, membrane samples should be stored in water in dark conditions to avoid drying and the occurrence of any unnecessary photochemical reactions.

## 1. Preparation of POM/polymer Composite Membrane

Note: The synthesis procedure follows that reported in the article by Helen *et al.*<sup>14</sup>, except that the amount of POM was altered.

1. Preparation of precursor polyvinyl alcohol (PVA) solution
  1. Add 3 g of polyvinyl alcohol 1000 (completely hydrolyzed) and a stirring bar to a 50 mL vial.
  2. Add 27 mL of water to the vial.
  3. Heat the vial to 70 °C within a water bath under stirring conditions to completely dissolve all polyvinyl alcohol particles.
2. Preparation of precursor polyacrylamide (PAM) solution
  1. Add 0.75 g of polyacrylamide (see **Table of Materials**) and a stirring bar to a 50 mL vial.
  2. Add 29.25 mL of water to the vial.
  3. Heat the vial to 70 °C within a water bath under stirring conditions to completely dissolve all polyacrylamide particles.
3. Preparation of mixture solution of POM and polymers
  1. Add 2 mL of PVA solution and 2 mL of PAM solution to a 50 mL vial.  
NOTE: As these polymer solutions have high viscosities, it is essential to accurately measure their volumes.
  2. Add a triangular-shaped stirring bar and 1 g of  $\text{H}_3\text{PW}_{12}\text{O}_{40}$  to the vial.  
CAUTION:  $\text{H}_3\text{PW}_{12}\text{O}_{40}$  is a highly acidic material and should be stored in refrigerator. When working with it, use plastic materials and not metal ones.
  3. Heat the vial to 70 °C within a water bath under vigorous stirring conditions and continue to stir for 6 h after leaching at 70 °C.
  4. Place a glass substrate (5 x 5 cm<sup>2</sup>) on a hot plate (approximately 100 °C) and drop 750  $\mu\text{L}$  of the solution onto the substrate.  
NOTE: The solution should be kept hot during the dropping process to prevent the polymers from congealing.
  5. To dry the sample, keep it overnight in a dark condition at room temperature.
4. Cross-linking process for membrane sample
  1. Add 72 mL of distilled water, 24 mL of acetone, 2 mL of 25% glutaraldehyde solution, and 2 mL of HCl to a 100 mL vial. This mixture is called the cross-linking reagent.
  2. Put the glass substrate with the sample in a Petri dish (approximately 9.5 cm diameter) and add the cross-linking reagent until the membrane is completely immersed.
  3. After 30 min, replace the cross-linking solution with distilled water, and wash once.
  4. Peel the membrane from the glass substrate using a spatula and store it in distilled water in dark conditions. This POM/polymer membrane is called POM/PVA/PAM.  
NOTE: If the membrane is used for the next process (reaction with donor metals or  $\text{MnO}_x$  deposition), the peeling-off process should be omitted.
  5. Use micro-Raman and FT-IR spectroscopy with POM/PVA/PAM to determine the chemical structure of the membrane<sup>13</sup>. Take an FT-IR spectrum of PVA/PAM (lacking POM) sample prepared by the same method as a reference.

## 2. Reaction of POM/polymer Membrane with Donor Metals ( $\text{Ce}^{3+}$ and $\text{Co}^{2+}$ )

1. Preparation of  $\text{Ce}^{3+}$  solution.
  1. Add 2.08 g of  $\text{Ce}(\text{NO}_3)_3 \cdot 6\text{H}_2\text{O}$  and a stirring bar to a 50 mL vial.
  2. Add 30 mL of water to the vial and stir to dissolve all  $\text{Ce}(\text{NO}_3)_3$ .
2. Reaction of membrane sample with  $\text{Ce}^{3+}$ 
  1. Put the membrane sample in a Petri dish (approximately 9.5 cm diameter) and add  $\text{Ce}^{3+}$  solution until the membrane is completely immersed.
  2. Put the Petri dish into a pre-heated oven at 80 °C for 5 h.
  3. Replace the  $\text{Ce}^{3+}$  solution with distilled water and wash once.
  4. Store in distilled water in dark conditions.
3. Preparation of  $\text{Co}^{2+}$  solution
  1. Use the same preparation and reaction procedures as with  $\text{Ce}^{3+}$ , except using 1.14 g of  $\text{CoCl}_2 \cdot 6\text{H}_2\text{O}$  instead of  $\text{Ce}(\text{NO}_3)_3 \cdot 6\text{H}_2\text{O}$ . Samples reacted with  $\text{Ce}^{3+}$  and  $\text{Co}^{2+}$  are called POM/PVA/PAM/Ce and POM/PVA/PAM/Co, respectively.
  2. In this study, micro-Raman spectra of POM/PVA/PAM/Ce and POM/PVA/PAM/Co were examined to determine the molecular structure of  $\text{PW}_{12}\text{O}_{40}^{3-}$  after reaction with donor metal ions<sup>13</sup>. The optical properties of these samples were also examined using UV-Vis spectroscopy.

### 3. Deposition of MnO<sub>x</sub> Water Oxidation Catalysts

NOTE: The preparation and deposition procedures of colloidal MnO<sub>x</sub> follow those in Perez-Benito *et al.* 1989<sup>15</sup> and Takashima *et al.* 2012<sup>16</sup>, respectively.

#### 1. Preparation of colloidal MnO<sub>x</sub> solution

1. Add 39.4 mg of KMnO<sub>4</sub> and a stirring bar to a 30 mL beaker.  
NOTE: CAUTION: KMnO<sub>4</sub> is a highly oxidative material; when working with it, use plastic spoons and not metal ones.
2. Add 10 mL water to the beaker and stir to completely dissolve all KMnO<sub>4</sub>.
3. Add 50 mg of Na<sub>2</sub>S<sub>2</sub>O<sub>3</sub>•5H<sub>2</sub>O and an oval-shaped stirring bar to a 500 mL round-bottom flask.
4. Add 20 mL water to the flask and stir to completely dissolve all Na<sub>2</sub>S<sub>2</sub>O<sub>3</sub>.
5. Add 10 mL of KMnO<sub>4</sub> solution to the flask drop-wise under vigorous stirring.  
Note: KMnO<sub>4</sub> solution should be added slowly to prevent formation of aggregated MnO<sub>2</sub>.
6. After adding the KMnO<sub>4</sub> solution, immediately add 470 mL of distilled water to the flask.
7. Keep stirring for over 2 h and then immediately use the solution for the next process (spraying).

#### 2. Spraying MnO<sub>x</sub> colloidal solution onto membrane sample

1. Place the membrane samples onto a hot plate (approximately 60 °C) with masks made of silicone rubber to determine the area to be used for deposition.  
NOTE: For the deposition of MnO<sub>x</sub> catalysts, the membrane samples should be placed on glass substrates. If the membranes have not been peeled off from the substrate, put them onto a hot plate as they are. Keep the surface of the membrane wet during the deposition process. The mask also works as a weight to prevent the membranes from flying off due to the high air pressure from the spray gun.
2. Add 300 mL of the colloidal MnO<sub>x</sub> solution to a 500 mL bottle connected to an automated spray gun (see **Table of Materials**) above the hot plate and spray the solution onto the membranes.
3. When the volume in the bottle decreases, add the remaining colloidal solution to the bottle.
4. Store the samples in distilled water in dark conditions. After MnO<sub>x</sub>-deposition, the samples are called POM/PVA/PAM/Ce/MnO<sub>x</sub> or POM/PVA/PAM/Co/MnO<sub>x</sub>.
5. Electron transfer properties under visible-light irradiation of POM/PVA/PAM/Co/MnO<sub>x</sub> were monitored using photoelectrochemical measurements at a particular electrode potential. To conduct the photoelectrochemical experiment, the membrane sample was fabricated on transparent Sn-doped In<sub>2</sub>O<sub>3</sub> (ITO) electrodes.

### Representative Results

Retention of the POM structure in the polymer matrix was confirmed by FT-IR and micro-Raman spectroscopy (**Figure 1**); vibration peaks corresponding to the Keggin structure of POM were observed, and peaks of the polymers were found to be shifted due to hydrogen bonding with POM. Spectroscopic analysis was very useful for determining successful construction of the charge transfer unit, and this was also confirmed by the apparent color change of the samples (**Figure 2**). It was also confirmed by UV-Vis spectroscopy and photoelectrochemical measurements (**Figure 3**), because charge transfer is achieved when all components are adequately aligned. In particular, the spectroscopic and photoelectrochemical results confirmed one directional charge transfer under light irradiation, which thus supports the validity of our synthetic method. The production of O<sub>2</sub> on MnO<sub>x</sub> was monitored using an indirect electrochemical method employing a rotating disk-ring electrode system, where the reduction current corresponding to O<sub>2</sub> reduction could be observed under light irradiation (**Figure 4**).

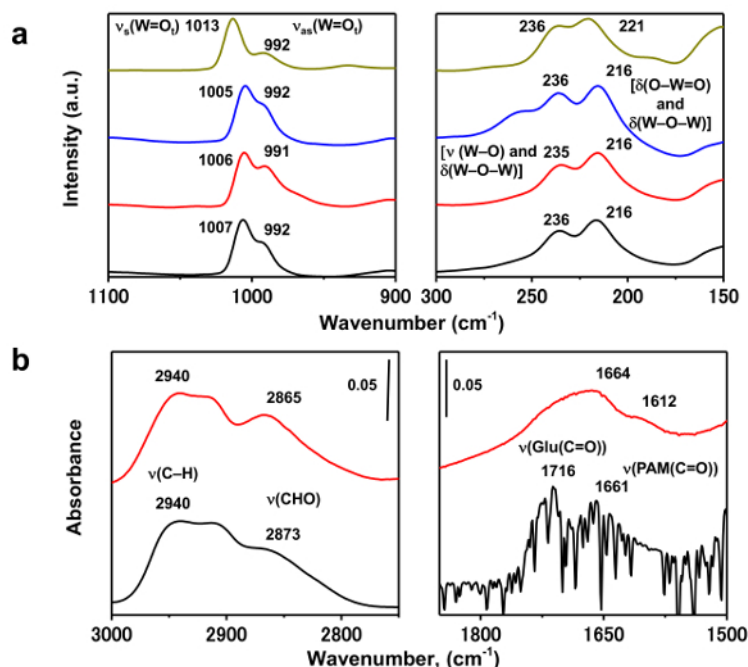


**Figure 1: Micro-Raman and FT-IR spectra.** (a) Micro-Raman spectra of membrane samples before (POM/PVA/PAM, black line) and after reaction with  $\text{Ce}(\text{NO}_3)_3$  (POM/PVA/PAM/Ce, red line) or  $\text{CoCl}_2$  (POM/PVA/PAM/Co, blue line). The spectrum of crystalline  $\text{H}_3\text{PW}_{12}\text{O}_{40}$  is also shown as a reference (dark yellow). A 532-nm laser with an intensity of 20 mW was used to irradiate the sample and obtain the spectra. (b) FT-IR spectra of POM-lacking sample (black line) and POM/PVA/PAM (red line) membrane samples. The samples were mounted in a homemade transmission IR vacuum cell equipped with KBr windows and their spectra were obtained in transmittance mode at room temperature with a deuterated triglycine sulfate detector. This figure has been modified with permission from Yamaguchi *et al.* 2017<sup>13</sup>, copyright 2017 American Chemical Society. [Please click here to view a larger version of this figure.](#)

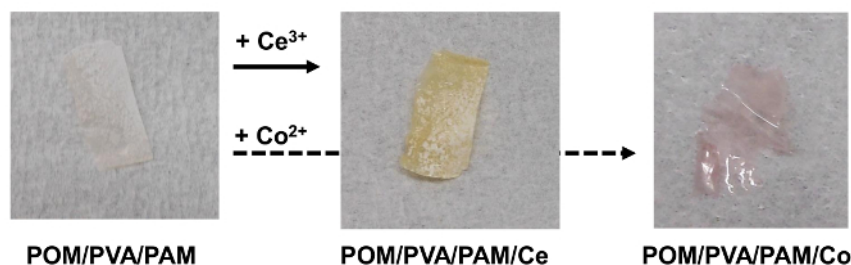


**Figure 2: Pictures of membrane samples.** Left: POM/PVA/PAM, center: POM/PVA/PAM/Ce, and right: POM/PVA/PAM/Co. [Please click here to view a larger version of this figure.](#)

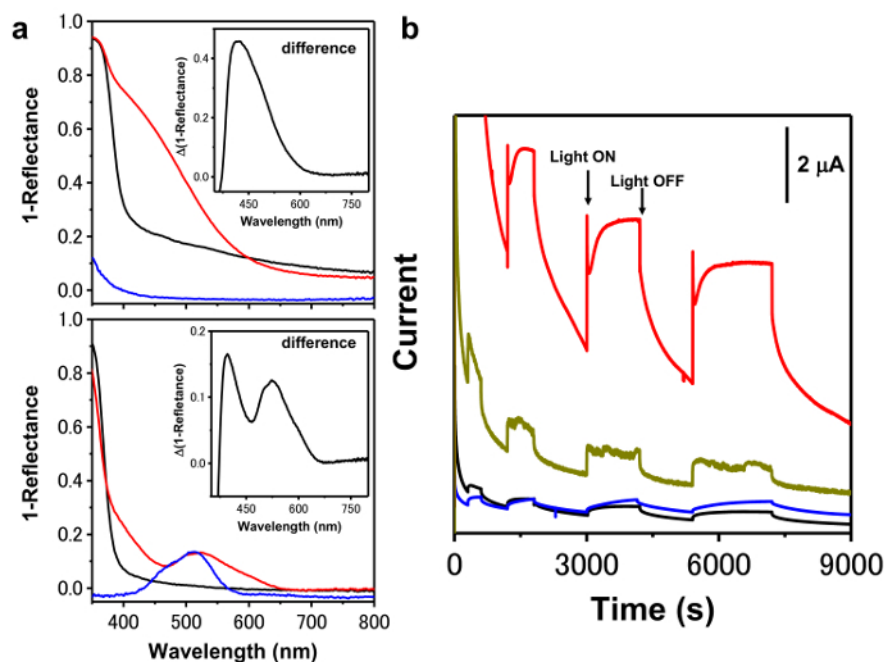


**Figure 3: UV-Vis diffuse reflectance spectra and I-t curves.** (a) Top: UV-Vis diffuse reflectance spectra of POM/PVA/PAM membrane samples before (black line) and after reaction with  $\text{Ce}(\text{NO}_3)_3$  (POM/PVA/PAM/Ce, red line). The spectrum of the POM-lacking membrane sample after reaction with  $\text{Ce}(\text{NO}_3)_3$  is also shown as a reference (blue line). Bottom: UV-Vis diffuse reflectance spectra of POM/PVA/PAM membrane samples before (black line) and after reaction with  $\text{CoCl}_2$  (POM/PVA/PAM/Co, red line). The POM-lacking membrane sample (PVA/PAM) did not react with  $\text{CoCl}_2$ ; therefore, the UV-Vis absorption spectrum of an aqueous solution of  $\text{CoCl}_2$  was used as a reference (blue line). The insets are subtraction spectra (after reaction minus before reaction). (b) I-t curves for (red line) POM/PVA/PAM/Co/MnO<sub>x</sub>, (dark yellow line) POM/PVA/PAM/Ce/MnO<sub>x</sub>, (black line) POM/PVA/PAM/Co, and (blue line) POM/PVA/PAM/MnO<sub>x</sub> samples fabricated on an ITO electrode and irradiated with visible-light after 20 min of Ar bubbling. The light source was a 300 W Xe lamp equipped with a 450 nm cutoff filter to prevent UV absorption. The electrolyte was 0.1 M  $\text{Na}_2\text{SO}_4$  (pH 10, adjusted with 1 M NaOH) and the applied potential was +1100 mV (vs a standard hydrogen electrode [SHE]). This figure has been modified from Yamaguchi *et al.* 2017<sup>13</sup>, copyright 2017 American Chemical Society. [Please click here to view a larger version of this figure.](#)

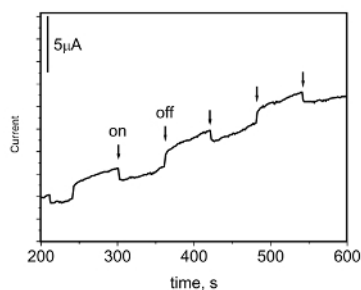


**Figure 4: I-t curves of ring part of rotating disk-ring electrode under photo irradiation.** POM/PVA/PAM/Co/MnO<sub>x</sub> was fabricated on the disk part. The rotating speed was 1500 rpm, and the disk and ring potential were maintained at 1120 mV and -280 mV vs SHE, respectively. [Please click here to view a larger version of this figure.](#)

## Discussion

It is critical to apply the cross-linking method introduced by Helen *et al.*<sup>14</sup> to develop a self-standing membrane. When polyvinyl acetate was applied as the base polymer in this study, aggregation of  $\text{H}_3\text{PW}_{12}\text{O}_{40}$  occurred, which prevented formation of the self-standing membrane. However, when fabrication of the membrane was attempted utilizing Nafion as the base polymer, there was no progression of the reaction with  $\text{Ce}^{3+}$  and  $\text{Co}^{2+}$ , although preparation of the self-standing membrane was achieved. In this study, to guarantee electron transfer throughout the membrane, the loading amount was modified to 80 wt%  $\text{H}_3\text{PW}_{12}\text{O}_{40}$  from that of 10 wt% heteropolyanions used in the work of Helen *et al.*<sup>14</sup>.

The micro-Raman spectra showed that the molecular structure of POM was highly retained in the polymer matrix both before and after the reaction with  $\text{Ce}^{3+}$  and  $\text{Co}^{2+}$ , as evidenced by the retention of Raman peaks characteristic for the Keggin structure of POM<sup>17</sup> (Figure 1a). FT-IR analysis confirmed that POM was successfully incorporated into the polymer matrix. Upon the reaction with POM, the vibration peaks corresponding to the functional groups of polymers<sup>14</sup> were found to be slightly shifted (Figure 1b), which indicates that POMs formed hydrogen-

bonding with the polymers. This hydrogen-bonding formation also supports the molecular dispersion of POM compared with crystalline  $\text{H}_3\text{PW}_{12}\text{O}_{40}$  without polymer matrix when the cross-linking process was used to avoid aggregation.

The step-by-step reaction of POM/PVA/PAM with  $\text{Ce}^{3+}$  and  $\text{Co}^{2+}$  enables a flexible choice of donor metals, which is an extremely important parameter for enabling desirable photochemical multi-electron transfer reactions. After reaction with the metals, the apparent colors of the samples changed from colorless to pale yellow (POM/PVA/PAM/Ce) and pink (POM/PVA/PAM/Co) (**Figure 2**). The UV-vis spectra showed new absorption in the visible region (**Figure 3a**), which is assigned to the metal-to-metal charge transfer (MMCT). It is of note that the absorption wavelength depends on the donor metals ( $\text{Ce}^{3+}$  for 420 nm and  $\text{Co}^{2+}$  for 395 nm; absorption at 530 nm in POM/PVAPAM/Co is assigned to d-d transition of  $\text{Co}^{2+}$ ), indicating that the absorption range can be controlled by modifying the donor metals.

The constructed MMCT systems possess the ability to photo-activate  $\text{MnO}_x$  water oxidation catalysts. Electron transfer by visible light irradiation was confirmed by photoelectrochemical measurements for POM/PVA/PAM/Ce/ $\text{MnO}_x$  or POM/PVA/PAM/Co/ $\text{MnO}_x$  fabricated on a Sn-doped  $\text{In}_2\text{O}_3$  (ITO) electrode. Photo-irradiation enhanced the current value in POM/PVA/PAM/Co/ $\text{MnO}_x$  and POM/PVA/PAM/Ce/ $\text{MnO}_x$ , while POM/PVA/PAM/Co and POM/PVA/PAM/ $\text{MnO}_x$  generated a negligible photo-current (**Figure 3b**). Visible-light irradiation of POM/PVA/PAM/Co/ $\text{MnO}_x$  induced MMCT ( $\text{Co}^{\text{II}} \rightarrow \text{W}^{\text{VI}}$ ) and the transfer of electrons at  $\text{PW}_{12}\text{O}_{40}^{3-}$  sites to the ITO electrode by intermolecular hopping between  $\text{PW}_{12}\text{O}_{40}^{3-}$  molecules. Furthermore, the generated holes at Co sites were transferred to  $\text{MnO}_x$ . Micro-Raman spectroscopy conducted after photoelectrochemical measurement showed that the POM structure was retained and that neither Ce nor Co oxide was formed, indicating that the sample was stable (at least over this experimental time scale). The photo-current difference between POM/PVA/PAM/Co/ $\text{MnO}_x$  and POM/PVA/PAM/Ce/ $\text{MnO}_x$  can be explained by the redox potential difference between  $\text{Ce}^{4+}/\text{Ce}^{3+}$  and  $\text{Co}^{3+}/\text{Co}^{2+}$  redox couples. Because the  $\text{Co}^{3+}/\text{Co}^{2+}$  couple possesses a greater positive redox potential than the  $\text{Ce}^{4+}/\text{Ce}^{3+}$  couple, it is advantageous to promote electron transfer from  $\text{MnO}_x$  to the Co site. This observation again emphasizes the importance of having a flexible choice of donor metals. Furthermore, in a previous study we showed that the redox potential of the acceptor site can be controlled by utilizing other types of POMs<sup>13</sup>, which expands the availability of this POM/polymer composite for the reaction field to promote both oxidation and reduction reactions.

To monitor the oxygen evolution reaction, we applied the electrochemical method using a rotating ring-disk electrode. The membrane sample was fabricated on the disk part of a ring-disk electrode, where the disk part was glassy carbon and the ring part was Pt. During photoelectrochemical measurements,  $\text{O}_2$  produced was reduced at the ring part, and reduction current was observed. **Figure 4** shows the increase in the reduction current in response to light irradiation. This result evidences that water oxidation was initiated on the surface of  $\text{MnO}_x$  under photo-illumination. The observed reduction current at the ring part was approximately 1  $\mu\text{A}$ , and the corresponding photo-current was approximately 2  $\mu\text{A}$ . As water oxidation on  $\text{MnO}_x$  is a four-electron process, and reduction of  $\text{O}_2$  on the ring part is a two-electron process, the coulombic efficiency of the photocurrent for water oxidation was thus almost 100%. In our experimental conditions, the applied overpotential was 460 mV. The reported activity of electrochemical OER on  $\text{MnO}_2$  by Meng *et al.*<sup>18</sup> was in the range of 0.5-0.7 V to reach a current density of 10  $\text{mA cm}^{-2}$  at pH = 13. Although we cannot compare these values, simply because the loaded amount and the surface area of  $\text{MnO}_x$  in our membrane system are unknown, the loading method and the OER activity of  $\text{MnO}_x$  itself should be improved in the future research.

This report demonstrates a method used to construct polyoxometalate-based MMCT units in a flexible polymer matrix by applying the cross-linking process. The limitation of this MMCT-based photoresponsive membrane is the weak absorption of visible light. Because the electronic interaction between metals in the MMCT unit is weak, the absorption coefficient of the oxo-bridged metal-based charge transfer system is generally small. Still, this system is advantageous compared with conventional semiconductor- or organic molecular-based photosensitizers in terms of the light durability and redox tuning to achieve product-separable photochemical systems. We utilize an electrode as an electron acceptor and  $\text{MnO}_x$  OER catalysts as a hole acceptor; however, this membrane system is also applicable for use in other catalytic systems where various redox reactions can be triggered by visible-light irradiation. We consider that this technique provides a new strategy for preparing a platform to construct a solar-to-chemical conversion system.

## Disclosures

The authors have nothing to disclose.

## Acknowledgements

A. Y. received financial support from the Global Center of Excellence for Mechanical Systems Innovation program of the University of Tokyo and from the University Tokyo Grant for Ph.D. Research. This work is partly supported by JSPS KAKENHI Grant-in-Aid for Young Scientists (B) (17K17718).

## References

1. Fujishima, A., Honda, K. Electrochemical Photolysis of Water at a Semiconductor Electrode. *Nature*. **238**, 37-38 (1972).
2. Nozik, A. J. Photoelectrochemistry: Applications to Solar Energy Conversion. *Annual Review of Physical Chemistry*. **29**, 189-222 (1978).
3. Bard, A. J., Fox, M.A. Artificial Photosynthesis: Solar Splitting of Water to Hydrogen and Oxygen. *Accounts of Chemical Research*. **28**, 141-145 (1995).
4. Lewis, N. S., Nocera, D. G. Powering the Planet: Chemical Challenges in Solar Energy Utilization. *Proceedings of the National Academy of Sciences of the United States of America*. **103**, 15729-15735 (2006).
5. Lin, W., Frei, H. Anchored Metal-to-Metal Charge-Transfer Chromophores in a Mesoporous Silicate Sieve for Visible-Light Activation of Titanium Centers. *The Journal of Physical Chemistry B*. **109**, 4929-4935 (2005).
6. Lin, W., Frei, H. Photochemical  $\text{CO}_2$  Splitting by Metal-to-Metal Charge-Transfer Excitation in Mesoporous  $\text{ZrCu}(\text{I})$ -MCM-41 Silicate Sieve. *Journal of the American Chemical Society*. **127**, 1610-1611 (2005).
7. Lin, W., Frei, H. Bimetallic redox sites for photochemical  $\text{CO}_2$  splitting in mesoporous silicate sieve. *Comptes Rendus Chimie*. **9**, 207-213 (2006).



8. Kim, W., Yuan, G., McClure, B. A., Frei, H. Light Induced Carbon Dioxide Reduction by Water at Binuclear  $\text{ZrOCo}^{\text{II}}$  Unit Coupled to Ir Oxide Nanocluster Catalyst. *Journal of the American Chemical Society*. **136**, 11034-11042 (2014).
9. Kim, W., Frei, H. Directed Assembly of Cuprous Oxide Nanocatalyst for  $\text{CO}_2$  Reduction Coupled to Heterobinuclear  $\text{ZrOCo}^{\text{II}}$  Light Absorber in Mesoporous Silica. *ACS Catalysis*. **5**, 5627-5635 (2015).
10. Takashima, T., Nakamura, R., Hashimoto, K. Visible Light Sensitive Metal Oxide Nanocluster Photocatalysts: Photo-Induced Charge Transfer from  $\text{Ce(III)}$  to Keggin-Type Polyoxotungstates. *The Journal of Physical Chemistry C*. **113**, 17247-17253 (2009).
11. Takashima, T., Yamaguchi, A., Hashimoto, K., Nakamura, R. Multielectron-transfer Reactions at Single  $\text{Cu(II)}$  Centers Embedded in Polyoxotungstates Driven by Photo-induced Metal-to-metal charge Transfer from Anchored  $\text{Ce(III)}$  to Framework  $\text{W(VI)}$ . *Chemical Communications*. **48**, 2964-2966 (2012).
12. Takashima, T., Nakamura, R., Hashimoto, K. Visible-Light-Absorbing Lindqvist-Type Polyoxometalates as Building Blocks for All-Inorganic Photosynthetic Assemblies. *Electrochemistry*. **79**, 783-786 (2011).
13. Yamaguchi, A., Takashima, T., Hashimoto, K., Nakamura, R. Design of Metal-to-metal Charge-transfer Chromophores for Visible-light Activation of Oxygen-Evolving Mn Oxide Catalysts in a Polymer Film. *Chemistry of Materials*. **29**, 7234-7242 (2017).
14. Helen, M., Viswanathan, B., Murthy, S. S. Poly(vinyl alcohol)-polyacrylamide Blends With Cesium Salts of Heteropolyacid as a Polymer Electrolyte for Direct Methanol Fuel Cell Applications. *Journal of Applied Polymer Science*. **116**, 3437-3447 (2010).
15. Perez-Benito, J. F., Brillas, E., Pouplana, R. Identification of a Soluble Form of Colloidal Manganese(IV). *Inorganic Chemistry*. **28**, 390 -392 (1989).
16. Takashima, T., Nakamura, R., Hashimoto, K. Mechanism of pH-Dependent Activity for Water Oxidation to Molecular Oxygen by  $\text{MnO}_2$  Electrocatalysts. *Journal of the American Chemical Society*. **134**, 1519-1527 (2012).
17. Bridgeman, A. J. Density Functional Study of the Vibrational Frequencies of  $\alpha$ -Keggin Heteropolyanions. *Chemical Physics*. **287**, 55-69 (2003).
18. Meng, Y., Song, W., Huang, H., Ren, Z., Chen, S.-Y., Suib, S. L. Structure-property Relationship of Bifunctional  $\text{MnO}_2$  Nanostructures: Highly Efficient, Ultra-stable Electrochemical Water Oxidation and Oxygen Reduction Reaction Catalysts Identified in Alkaline Media. *Journal of the American Chemical Society*. **136**, 11452-11464 (2014).